Agricultural and Forest Meteorology 194 (2014) 175–187

Contents lists available at ScienceDirect

Agricultural and Forest Meteorology

journal homepage: www.elsevier.com/locate/agrformet

# Changes in fluxes of heat, $H_2O$, and $CO_2$ caused by a large wind farm

Daniel A. Rajewski[a,*], Eugene S. Takle[a], Julie K. Lundquist[b,c], John H. Prueger[d], Richard L. Pfeiffer[d], Jerry L. Hatfield[d], Kristopher K. Spoth[a], Russell K. Doorenbos[a]

[a] Department of Agronomy, Iowa State University, Ames, IA 50011, USA
[b] Department of Atmospheric and Oceanic Sciences, University of Colorado, Boulder, CO 80309, USA
[c] National Renewable Energy Laboratory, Golden, CO 80401, USA
[d] National Laboratory for Agriculture and the Environment, Ames, IA 50011, USA

ARTICLE INFO

*Article history:*
Received 2 October 2013
Received in revised form 13 March 2014
Accepted 29 March 2014
Available online 13 May 2014

*Keywords:*
Surface fluxes
Wind turbines
Turbulence
Crop microclimate
Spectral analysis

ABSTRACT

The Crop Wind-Energy Experiment (CWEX) provides a platform to investigate the effect of wind turbines and large wind farms on surface fluxes of momentum, heat, moisture, and carbon dioxide ($CO_2$). In 2010 and 2011, eddy covariance flux stations were installed between two lines of turbines at the southwest edge of a large Iowa wind farm from late June to early September. We report changes in fluxes of momentum, sensible heat, latent heat, and $CO_2$ above a corn canopy after surface air had passed through a single line of turbines. In 2010, our flux stations were placed within a field with homogeneous land management practices (same tillage, cultivar, chemical treatments). We stratify the data according to wind direction, diurnal condition, and turbine operational status. Within these categories, the downwind–upwind flux differences quantify turbine influences at the crop surface. Flux differences were negligible in both westerly wind conditions and when the turbines were non operational. When the flow is perpendicular (southerly) or slightly oblique (southwesterly) to the row of turbines during the day, fluxes of $CO_2$ and water ($H_2O$) are enhanced by a factor of five in the lee of the turbines (from three to five turbine diameter distances downwind from the tower) as compared to a west wind. However, we observe a smaller $CO_2$ flux increase of 30–40% for these same wind directions when the turbines are off. In the nighttime, there is strong statistical significance that turbine wakes enhance upward $CO_2$ fluxes and entrain sensible heat toward the crop. The direction of the scalar flux perturbation seems closely associated to the differences in canopy friction velocity. Spectra and co-spectra of momentum components and co-spectra of heat also demonstrate nighttime influence of the wind turbine turbulence at the downwind station.



## 1. Introduction

Large wind farms have been constructed across the U.S. Midwest over the last decade, and this expansion is likely to continue (U.S. DOE, 2008; AWEA, 2012). Much of the land used for turbines in the Midwest also is managed for agricultural purposes in ways that influence roughness height and surface fluxes of heat and moisture. It is likely that management practices such as tillage, crop-type, cultivar, plant density, and chemical application can influence turbine hub-height speed through changes in turbulent coupling. For instance, Barthelmie (1999), Emeis (2010), and Stull (1988) describe how surface roughness regulates near-surface wind profiles. Further, Pichugina et al. (2005) and Storm and Basu (2010) discuss surface influences on nighttime speed and directional shear characteristics below and within the turbine rotor layer. Weather prediction models that have parameterizations for wind turbines suggest that the turbines affect near-surface winds, temperature, and moisture (Baidya Roy et al., 2004; Baidya Roy, 2011; Fitch et al., 2012; Fitch et al., 2013a, 2013b; Wang and Prinn, 2010). A recent paper (Armstrong et al., 2014) has identified a range of potential microclimate and soil effects of wind farms.

Based on experience quantifying flow characteristics around shelterbelts (Wang and Takle, 1995; Wang et al., 2001), wind turbines are expected to modify the mean and turbulence characteristics of a uniform boundary layer above a crop canopy surface. As a bluff obstacle to the wind, the rotor blades, nacelle, and tower create a localized perturbed pressure field that affects mean flow from the surface to well above the blade diameter. Wind speed reduction and small-scale turbulence created by flow past the blades and nacelle form a wake region that can influence the surface indirectly (by decoupling ambient flow aloft from near-surface

* Corresponding author at: Iowa State University, 3132 Agronomy Hall Ames, IA 50011, USA. Tel.: +1 515 294 9384.
*E-mail address:* drajewsk@iastate.edu (D.A. Rajewski).

http://dx.doi.org/10.1016/j.agrformet.2014.03.023

flow and by creating waves and pressure fluctuations that are mediated to the surface) and directly when the wake reaches the surface (Rajewski et al., 2013). Exchanges of heat, $H_2O$, and $CO_2$ with crops are affected by these changes introduced in the lee of the turbines. The magnitude and locations of these changes are controlled by the turbine characteristics (hub height, rotor diameter, blade style, blade pitch angle, and model-specific thrust and power coefficients) and the ambient conditions (atmospheric stability, wind direction, wind speed, and moisture conditions). The field measurements reported herein quantify fluxes and offer opportunities for verifying numerical and conceptual models of surface fluxes of sensible and latent heat, and gaseous constituents such as $CO_2$.

Several numerical simulations of large wind farms demonstrate increased daytime evapotranspiration up to 0.4 mm day$^{-1}$ or about 10 W m$^{-2}$, higher nighttime temperatures (0.5–2 °C), and enhanced downward sensible heat flux of 5 W m$^{-2}$ to 10 W m$^{-2}$ (Adams and Keith, 2007; Baidya Roy, 2004, 2011; Baidya Roy and Traiteur, 2010; Cevarich and Baidya Roy, 2013; Fitch et al., 2013a). Large-eddy simulation (LES) and 1*D* surface layer models with wind turbine parameterizations also indicate a 10–15% increase in scalar fluxes in the surface layer below the turbines (Calaf et al., 2011). Wind tunnel studies by Zhang et al. (2012, 2013) of wind turbine arrays in neutral or convective boundary layers depict increased heat flux (up to 24%) immediately around the downwind side of each tower base. From a simulation of turbine wakes during a steady-state stably-stratified period, Lu and Porté-Agel (2011) determine that the downward sensible heat flux is reduced 14–27% of the ambient flux deep within a wind farm array but there is no change in either the surface temperature, nor in the potential temperature profile up to the bottom tip of the turbine rotor.

A few observational studies, primarily using remote sensing techniques instead of in-situ measurements, show how large wind farms can perturb crop microclimate conditions. Zhou et al. (2012a, 2012b) used MODIS satellite data to determine that temperatures were 0.5–0.7 °C warmer in the years following construction of several west Texas wind farms. The study documented slight increases in surface albedo and decreases in surface vegetative fraction for each turbine construction "footprint." However, the authors did not report field-scale characteristics related to soils, changes in land use such as rangeland or agricultural activities. Another satellite analysis by Walsh-Thomas et al. (2012) documented similar or more extensive warming from 1982 to 2011 over the San Gorgonio wind farm in California, but the study area was influenced by terrain-induced changes in temperature that may have obscured the specific contribution of the wind farm to changes in surface temperature. Air temperature, relative humidity, and evaporation differences were noted among five surface stations positioned within a 300-turbine wind farm in Western Indiana during the 2011 post harvest period (Henschen et al., 2011). Unfortunately, no microclimate measurements were provided of undisturbed conditions outside the wind farm. Furthermore, the authors do not describe inherent field-scale variability that may have been caused by land management (e.g. tillage) or soil factors (e.g. temperature, moisture, texture, drainage). Another study in a wind farm located in the U.S. Midwest (Barthelmie et al., 2013; Smith et al., 2013) depicts a weakening nocturnal inversion strength in 80–2 m vertical temperature gradient when turbine wakes are influencing the surface. Measurements were collected over a smooth landscape ($z_0$ = 0.05 m) before the 2012 crop was planted.

Rajewski et al. (2013) suggested that the first step in determining whether turbines influence agricultural crop growth and yield is to determine if influences in key fluxes and canopy flow by wind farms and wind turbines are measureable above natural variations. To address this question we conducted two field measurement campaigns within a large utility scale wind farm in central Iowa during the 2010 and 2011 Crop Wind-Energy Experiment (CWEX-10/11). In this report we specifically address how the wind turbine flow perturbations affect fluxes of heat, moisture, and $CO_2$. In Section 2, we present a brief summary of the relevant measurements. In Section 3, we discuss the analyses used to determine the flux differences for turbine-influenced and no-turbine-influenced conditions. Section 4 highlights the results of the flux analysis using conditional binning for several factors (e.g. day/night, wind direction, turbine operational status). We summarize the results in Section 5 and offer additional objectives for future experiments to quantify the influence of wind turbines/large wind farms on crops.

## 2. Materials and methods

Flux measurements were made during summers of 2010 and 2011 in the southwest portion of an Iowa wind farm consisting of 1.5-MW turbines with 37 m long blades, and hub height of 80 m. A detailed description of the CWEX deployments is provided in Rajewski et al. (2013). According to the U.S. Department of Agriculture Natural Resources Conservation Service (USDA-NRCS) soil maps (http://ortho.gis.iastate.edu), our study area included six different loamy soils speckled throughout the study area, each with different water retention and drainage characteristics. Although soil conditions will influence fluxes, crop management practices are also influential. In this report we seek to demonstrate flux changes over and above natural variability due to soil conditions. Because flux stations in 2011 were located in corn fields having different management practices, the present investigation is focused on 2010 data to eliminate influence of crop management practices on flux differences.

The National Laboratory for Agriculture and the Environment (NLAE) provided instruments and data collection for four flux stations in 2010. The University of Colorado (CU) and the National Renewable Energy Laboratory (NREL) provided a wind profiling light detection and ranging (LiDAR) system downwind of the turbines in 2010 (Aitken et al., 2012) but the LiDAR data was only available for a small subset of the measurement period and therefore is not incorporated into the present analysis of the surface flux data. In 2010, our stations measured fluxes upwind and downwind (prevailing wind being from the south) of a line of turbines from 30 June to 7 September. The reference upwind flux station [NLAE 1] was positioned about 330 m (4.5 *D*) south of the first line of turbines (denoted as the B turbine line), and the first downwind station [NLAE 2] was located 175 m (2.4 *D*) north of the B turbine line. Additional stations [NLAE 3] and [NLAE 4] were located 1.3 km (17.5 *D*) and 2.5 km (33.8 *D*) north of the B-line. NLAE 4 was about 650 m (8.8 *D*) north of a second turbine line, designated as the A line, which provided influences of two lines of turbines for some southerly wind directions. However, only NLAE 1 and NLAE 2 measured concentrations of $H_2O$ and $CO_2$, and so we restrict our analysis in this report to these stations.

CSAT3 sonic anemometers (*Campbell Scientific*, *Logan*, *Utah*) and LI-7500 gas analyzers (*Li-Cor*, *Lincoln*, *Nebraska*) were installed at 6.5 m above the soil surface. QREBS7.1 net radiometers (*REBS, Inc., Bellevue, WA*) were additionally located at the 6.5 m height for calculation of the surface energy balance, however there were no sensors installed within the soil. A tipping bucket rain gage (*Texas Electronics*, *Dallas*, *TX*) filtered poor-quality data periods and additional temperature and relative humidity probes (*HMP-45 C*, *Vaisala*, *Helsinki*, *Finland*) installed at 9-m and 5-m above the surface were used to calculate mean air density for the moisture correction

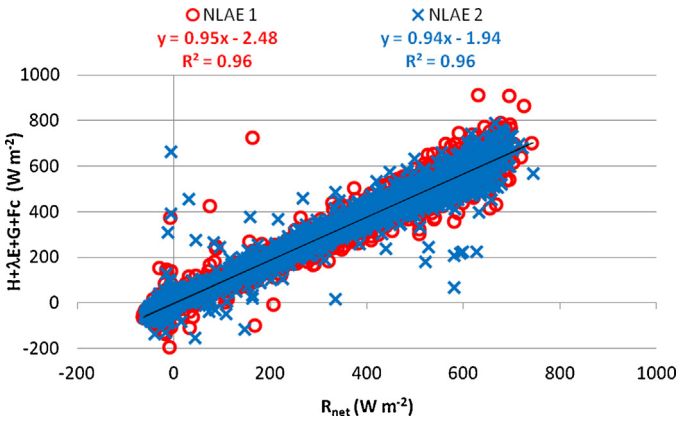


**Fig. 1.** Energy budget closure trend line and correlation coefficient ($R^2$) of ($R_{net} - G$ vs. $H + \lambda E + F_c$) among the upwind and downwind flux stations NLAE 1 and NLAE 2.

to the sensible, latent, and $CO_2$ fluxes. At installation in late June, the corn crop measured approximately 1.8 m, growing to a maximum height of 2.8 m in the middle of July. The surface roughness varied between 0.1 and 0.4 m approximately estimated as one-tenth of the canopy height (Campbell and Norman, 1998).

Eddy covariance fluxes are calculated for each 30-min intervals based on 20-Hz time series from the sonic anemometers and the gas analyzers. Corrections were applied to the sonic anemometer tilt angle (Wilczak et al., 2001), virtual temperature (without the tilt angle) (Schotanus et al., 1983), and to the $H_2O$ and $CO_2$ concentrations from the gas analyzer according to Webb et al. (1980). Data taken during precipitation events and data from periods having missing values from both the upwind or downwind stations were eliminated (about 19%). We also performed a quality control of the temperature profile measurements at 9 m and 5 m during which we rejected all events (an additional 2%) where $T_{NLAE\ 2} - T_{NLAE\ 1} > |5\ ^\circ C|$ since the temperature and relative humidity profile measurements were used in air density calculation for the corrected fluxes.

## 3. Calculations

### 3.1. Surface energy budget considerations

We define the surface energy balance equation as in Leuning et al. (2012) but with slightly rearranged form:

$$R_{net} - G = H + \lambda E + F_c + F_b \quad (1)$$

where $R_{net}$ is the net radiation, $G$ is the soil heat flux, $H$ is the sensible heat flux, $\lambda E$ is latent heat of evapotranspiration, $F_c$ is the energy absorbed/released by $CO_2$, and $F_b$ is the thermal storage within the crop canopy elements (e.g. leaves, stems, reproductive matter). $H$, $\lambda E$, $F_c$, and $R_{net}$ were measured, but we did not measure $G$ and $F_b$. We therefore parameterize $G$ as a daytime or nighttime fraction (0.1 or 0.5, respectively)*$R_{net}$ (e.g. Stull, 1988). We could not determine $F_b$ in the absence of biomass measurements. Canopy storage of heat may be significant to energy closure during several morning hours after sunrise (e.g. Meyers and Hollinger, 2004). However, we estimated this term to be small (<2 W m$^{-2}$) and therefore neglected $F_b$ in our energy budget. Leuning et al. (2012) defines $F_c$ (the energy flux of $CO_2$) as $F_c = f_c^* - 0.489$, where the constant is the $CO_2$ absorption determined by Blanken et al. (1997), and $f_c$ is the corrected vertical flux of $CO_2$. The scatter plot of the energy terms ($R_{net} - G$ vs. $H + \lambda E + F_c$) in Fig. 1 for NLAE 1 and NLAE 2 demonstrated about 95% energy closure. We attribute the satisfactory agreement in our energy budget to using the most updated flux-correction procedures, especially accounting for greater flux capture when using the sonic tilt corrections (Leuning et al., 2012; Wilczak et al., 2001).

### 3.2. Selection of periods for creating composites

We calculate the differences of the energy flux of $H$, $\lambda E$, and $f_c$ between the NLAE 2 (downwind of turbine line B) and NLAE 1 (upwind of turbine line B) stations. We analyze the aerodynamic differences between the two stations by comparing the friction velocity ($u_*$). Each 30-minute time period is classified by the following characteristics: turbine operating status (OFF/ON), surface wind direction, and thermal stratification. We determine turbine operational periods from the turbine Supervisory Control And Data Acquisition (SCADA) data from turbines in the B line. The SCADA nacelle wind speed and instantaneous power are reported in 10-min intervals which we then average to 30-min values to compare to fluxes. We define ON periods as periods when the average power produced by each turbine is greater than 100kW or when the turbine nacelle speed is at or greater than 5 m s$^{-1}$. OFF periods are defined as periods when the average power is at or below 0 kW. We compare power values among the three western-most turbines (B1, B2, and B3) in the B line to determine when all turbines were ON or all turbines were OFF. Surface flux reports are eliminated for periods (about 17%) when the SCADA data reveal a combination of some turbines operating and others not. We consider only periods having wind directions that allow turbines B1-B3 to influence our stations.

We find it important to consider both turbine power production and wind speed to quantify turbine status. Turbines may not be turning or in a low power operating state due to low wind speeds. Turbines also may be shut down for maintenance, for safety concerns during a thunderstorm, or when lightning is detected in the vicinity of the wind farm. Even when the turbine is OFF, turbines may influence fluxes because the blades, nacelle and tower create an obstacle to boundary layer flow. Vortices around the blades and towers, albeit small (e.g. Vermeer et al., 2003), may influence flux measurements, especially for northerly flow conditions when several lines of turbine wakes are contributing to flux perturbations at the southeast edge of the wind farm.

Each 30-minute period is additionally classified according to the downwind (NLAE 2) flux station wind direction. Waked or non-waked wind directions from the flux tower are determined by using an assumption of a 5° expansion of wakes from the turbine rotor as observed by Barthelmie et al. (2010) and adopted in the analysis of Rajewski et al. (2013). Fig. 2 presents a graphical interpretation of these wake-direction sectors for each wind turbine over the NLAE 2 flux station. In this study we use winds from WSW, SW, SSW, and S-SSE to evaluate influence of turbines B1-B3 on fluxes measured at NLAE 1. West winds (WEST) provide conditions where fluxes at NLAE 1 and NLAE 2 would be identical except for possible instrument bias or differences in fetch conditions for these two locations. We omit periods having all other wind directions.

We further limit our analysis to daytime and nighttime subperiods when surface radiation conditions are not changing rapidly. We classify a daytime period, DAY, to be when the net radiation from NLAE 1 $R_{net} > 300$ W m$^{-2}$ and a nighttime period, NIGHT, when $R_{net} < 0$ W m$^{-2}$. We acknowledge that boundary layer-transition and cloudy periods contribute to crop fluxes, but our goal was to create ensembles of clearly daytime and nighttime periods when fluxes were not changing rapidly due to diurnal or cloudiness effects. 2010 was a wet year so there are fewer opportunities for comparisons based on some specific atmospheric conditions (daytime cloudy vs. daytime clear etc.).

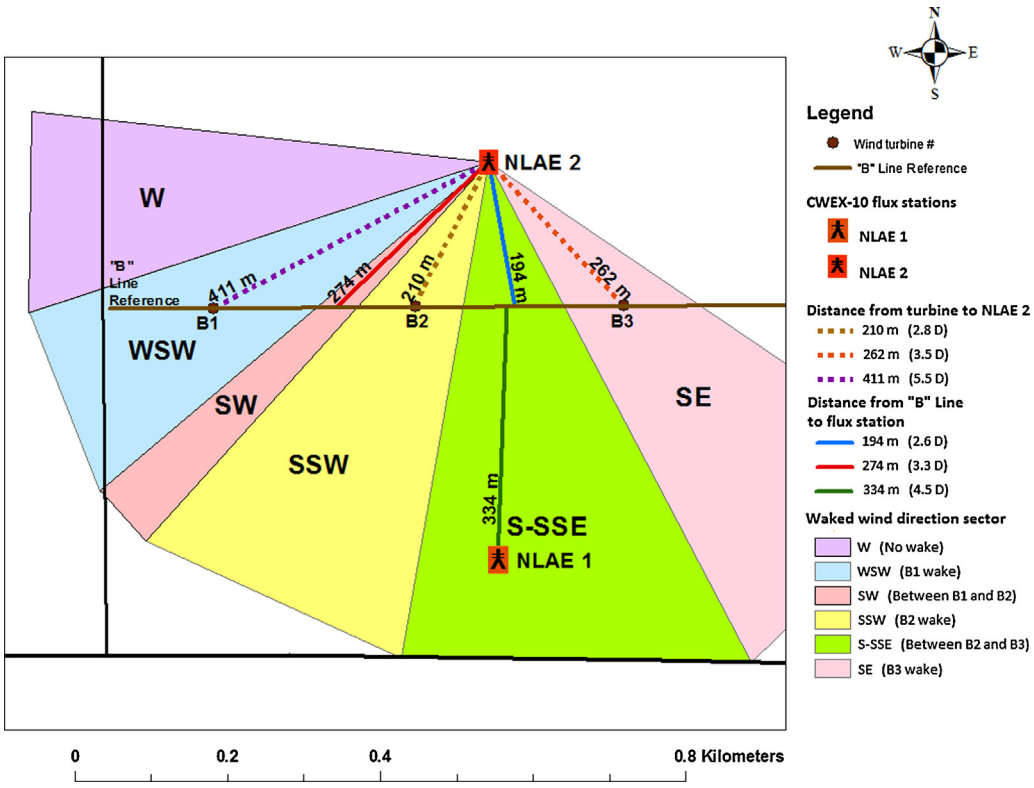


**Fig. 2.** Graphical representation of B-line of turbine wake wind direction sectors for the downwind flux tower (NLAE 2) overlain on the CWEX-10 measurement locations. These directional categories are represented in the flux difference directional day and nighttime composites.

### 3.3. Analyses of the flux differences composites

We first demonstrate a diurnal range of the flux differences by comparing all wind direction and thermal stratifications when the turbines are ON vs. OFF. Our mean differences in the flux are displayed in Figs. 3–7 in addition to 95% confidence intervals of the flux difference. The confidence intervals of the mean difference are applied analogously to the *t*-test and Wilcoxon signed Rank tests in detecting turbine impacts of air temperature within large wind farms in Texas (Zhou et al., 2012a) and in California by Baidya Roy and Traituer (2010).

Secondly we present differences in the fluxes according to typical DAY and NIGHT periods for the aforementioned wake direction indicators from the NLAE 2 station. Table 1 indicates the number of observations collected for each 30 min period with the turbines in the ON and OFF state, ($\Sigma$ON, $\Sigma$OFF) the individual turbine direction indicator categories in the on and off state (e.g. B2_ON (SSW), B2_OFF (SSW)), and the no-wake westerly categories for the individual events with the turbines operational (WEST_ON) and offline (WEST_OFF).

Thirdly we examine the differences in the NLAE 1 and NLAE 2 turbulence transfer efficiencies for each of the fluxes for the ON/OFF comparisons according to the reference thermal stability category at NLAE 1 and the waked wind direction category at NLAE 2. We determine the stability category at the reference NLAE 1 station by adopting the classification in Rajewski et al. (2013): NEUTRAL for $-0.05 \le z/L \le 0.05$, UNSTABLE as $z/L < -0.05$, and STABLE as $z/L > 0.05$. The turbulence transfer efficiency is a measure of the intensity of the turbulence exchange with the surface. We denote for the composite of the $u$ and $v$ vertical momentum flux in the momentum turbulence transfer efficiency as:

$$\chi u_*^2 = \frac{u_*^2}{\sqrt{(\sigma_u^2 + \sigma_v^2)} \times \sigma_w} \tag{2}$$

and similar formulation is derived for the turbulence efficiency for the heat, moisture, and $CO_2$ fluxes (e.g. Roth and Oke, 1995; Moriwaki et al., 2002):

$$\chi_{wT} = \frac{\overline{w'T'}}{\sigma_w \times \sigma_T}, \tag{3}$$

$$\chi_{wq} = \frac{\overline{w'q'}}{\sigma_w \times \sigma_q}, \tag{4}$$

$$\chi_{fc} = \frac{\overline{w'c'}}{\sigma_w \times \sigma_c}, \tag{5}$$

### 3.4. Spectral analysis detection of turbine perturbation of crop fluxes

One specific time period enables exploration of the spectral response of surface momentum and heat to the turbine impact. During the overnight hours of 27–28 August 2010, hub height winds (as reported by the turbine) were southerly while the reference NLAE 1 station reported south-south-easterly winds, while the turbines were ON from 21:00 to 22:00 LST and OFF for 50-min between 23:00 and 00:00 LST. We compare the power spectra and co-spectra in the ON vs. OFF events for the $v$-component of variance ($\overline{v'v'}$), the vertical velocity variance ($\overline{w'w'}$), the vertical turbulent momentum flux ($\overline{v'w'}$) and vertical turbulent heat flux ($\overline{w'T'}$). Power spectra $fS_v$, $fS_w$ and the co-spectra $fCO_{vw}$ intensities are normalized by the reference $u_*^2$. Similarly for the co-spectra of heat ($fCO_{wT}$) we normalize by the reference $T_*^2$ where ($T_* = -H/u_*$). For a like manner on the horizontal axis we normalize the frequency by the wind speed (near 2.0 m/s) at the measurement height (6.5 m) to visualize the relative energy scale responsible for each portion of the spectra/co-spectra. The peak spectral intensity and the related normalized frequency are identified at NLAE 1 and NLAE 2 for ease in depicting the turbine impact on the fluxes for the ON and OFF cases.

**Table 1**
Wind direction sectors corresponding to the turbine wake or gap (between turbine) flow for the B1 to B3 turbines on the leading line of turbines at the wind farm. Composites of these direction sectors are included for when the turbines were operational or offline. The number of observations in the DAY and NIGHT cases is included.

| Case direction category | Turbine wake Indicator and wake wind directions | Sample size (N) DAY | Sample size (N) NIGHT |
|---|---|---|---|
| B1_ON (WSW) | B1 (5.5*D* to turbine, 229°-251°) | 17 | 38 |
| B12G_ON (SW) | gap between B1 and B2 (3.3*D* to line, 221°-229°) | 26 | 16 |
| B2_ON (SSW) | B2 (2.8*D* to turbine, 189°-221°) | 67 | 54 |
| B23G_ON (S-SSE) | gap between B2 and B3 (2.6*D* to line, 151°-189°) | 160 | 406 |
| ∑ON | (combination turbines operating) | 270 | 514 |
| WEST_ON | (Westerly no-wake, 251°-285°) | 38 | 78 |
| B1_OFF (WSW) | B1 (5.5D to turbine, 229°-251°) | 6 | 11 |
| B12G_OFF (SW) | gap between B1 and B2 (3.3D to line, 221°-229°) | 4 | 3 |
| B2_OFF (SSW) | B2 (2.8D to turbine, 189°-221°) | 23 | 19 |
| B23G_OFF (S-SSE) | gap between B2 and B3 (2.6D to line, 151°-229°) | 57 | 47 |
| ∑OFF | (combination turbines offline) | 90 | 80 |
| WEST_OFF | (Westerly no-wake, 251°-285°) | 38 | 30 |

## 4. Results

### 4.1. Mean flux difference composites

#### 4.1.1. Friction velocity

The downwind–upwind difference in friction velocity as a function of time of day depicts a significant impact of turbine operation

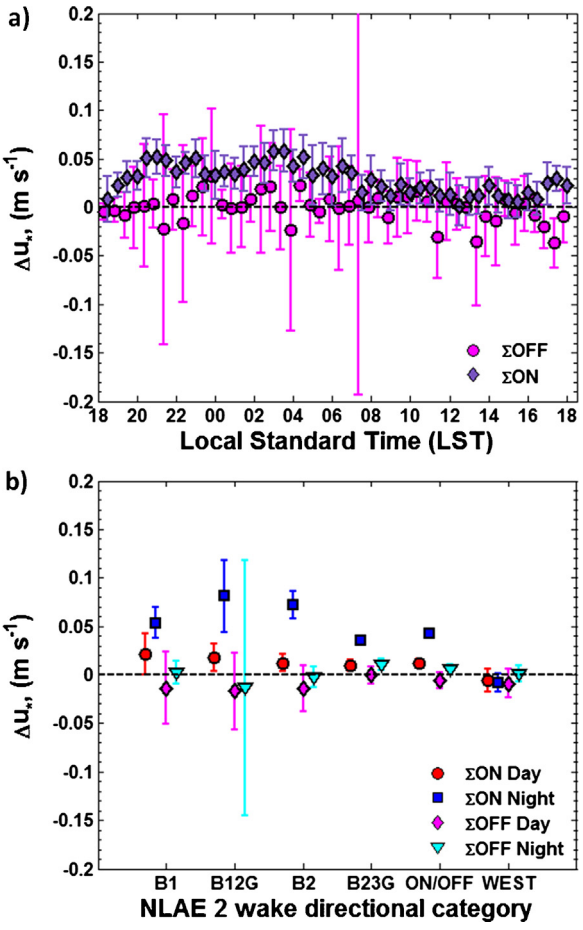


**Fig. 3.** (a) Downwind–upwind mean differences and 95% confidence intervals in friction velocity ($u_*$) for turbines ON and turbines OFF in a diurnal period. (b) Wind direction-turbine wake sector downwind–upwind mean differences and 95% confidence intervals in $u_*$ for the DAY and the NIGHT case.

(Fig. 3a), especially at night. We observe nearly a 25–50% increase in $u_*$ at NLAE 2 during nighttime hours while turbines are ON as apposed to OFF. In the daytime, however more ambiguity exists, likely due to strong daytime mixing.

When the turbines are OFF, the daytime difference in $u_*$ at the downwind station is negligible or at most a few percent decrease ($u_{*\mathrm{NLAE\ 1}} = 0.3\ \mathrm{m\,s^{-1}}$), with a slight increase ($u_{*\mathrm{NLAE\ 1}} = 0.5\ \mathrm{m\,s^{-1}}$) when the turbines are ON. The turbines have a much stronger effect at night than during the day, and when they are ON as opposed to OFF (Fig. 3b). During westerly cases, when flow is parallel to the row of turbines and the turbines affect neither flux station, no differences in friction velocity are apparent. These ranges of daytime differences (less than 10%) for westerly winds may be negligible for comparison to numerical or wind tunnel simulations but the flux perturbation is 40 times the measurement resolution of the sonic anemometer (e.g. Campbell Scientific, 2014). In the OFF condition the slight decrease of canopy mixing in southwesterly flow may indicate the impact of the perturbation pressure field around the B1 and B2 turbines although the turbine blades remain stationary (Rajewski et al., 2013).

The highest increase in canopy mixing (25-70%) occurs at night, between the wakes of turbines B1 and B2 and within the B2 wake. In contrast, westerly flow cases and the turbines OFF condition demonstrate <5% higher friction velocity at NLAE 2. For the ON condition, $u_*$ increases slightly (<10%) for southerly flow between turbines B2 and B3. Slightly larger $u_*$ is also occurs when the B1 turbine wake is overhead of the downwind station. The larger variability markers at these waked or between wake flow categories than for the southerly flow case between the B2 and B3 turbines is related to a smaller sample of observations. We note small to negligible decreases in canopy mixing at NLAE 2 in nocturnal periods with the turbines OFF for flow between the B1 and B2 turbines. These observations, marked with substantial variability, we attribute to a smaller sample size, the intermittency of turbulence, and episodic Kelvin Helmholtz instability.

#### 4.1.2. Sensible heat flux

In the heat flux differences (Fig. 4a), we observe a uniform but weak downward transport of heat at NLAE 2 for the late evening and first few hours after sunset when the turbines are operational. The 5–10 $\mathrm{W\,m^{-2}}$ departure of flux likely corresponds to the growth of the stable boundary layer into the layer of air between the top and bottom of the turbine blades. We indicate the strongest influence

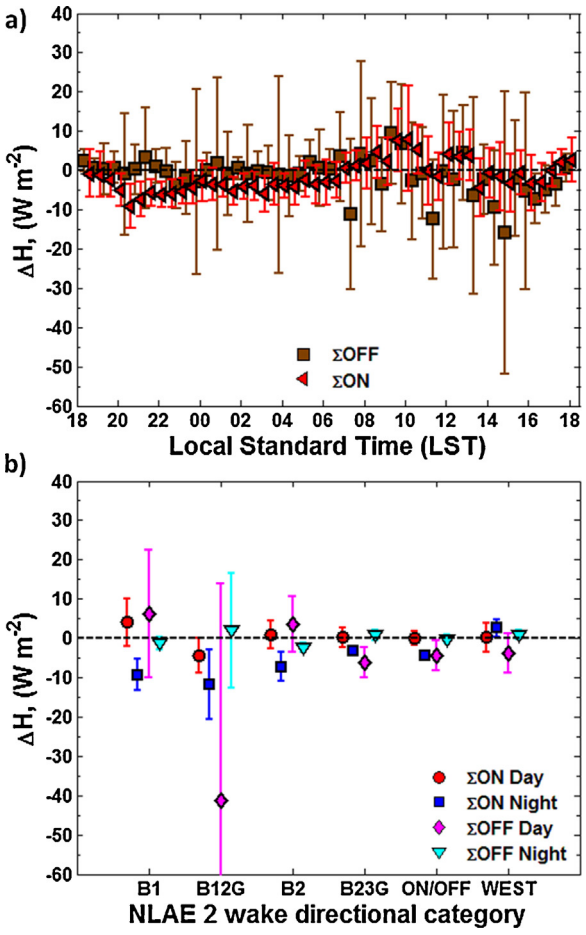


**Fig. 4.** As in Fig. 3 but for sensible heat flux ($H$).

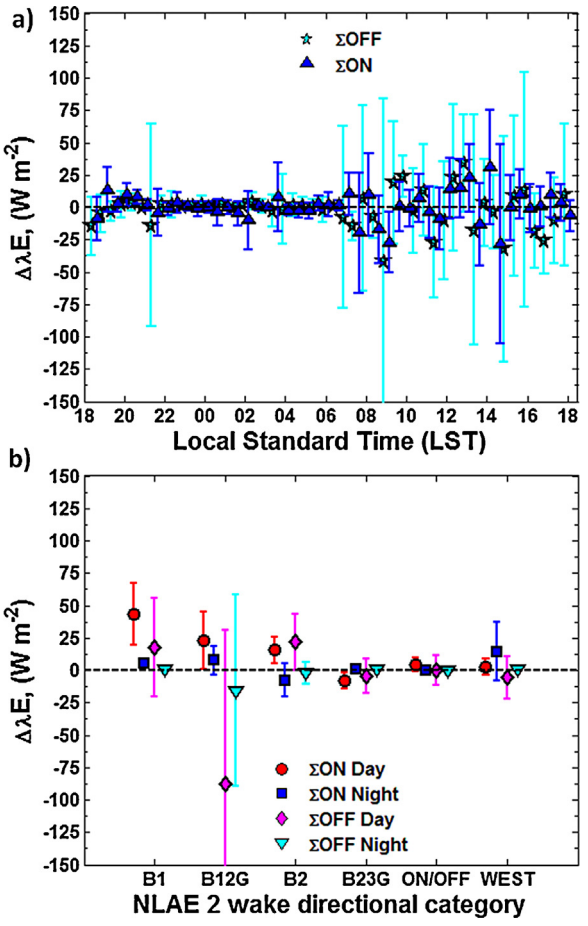


**Fig. 5.** As in Fig. 3 but for latent heat flux ($\lambda E$).

of the turbine when the ambient scales of turbulence are on the order of the size of the turbine blades (0.5–1.0$D$). In the last half of the night there is weaker flux difference and we refer to our previous investigation of low level jets as a possible mechanism to dilute the turbine transport of downward heat flux (e.g. Rajewski et al., 2013; Rhodes and Lundquist, 2013). In the daytime we observe a similar amount of surface cooling of less than 10 W m$^{-2}$ during the breakup of the temperature inversion when the ambient scales of mixing are the size of the turbine rotor. Flux differences are more variable in the other afternoon periods and for the majority of the day and night hours when the turbines are OFF. Nighttime intermittency in scalar flux is expected whereas in the daytime, moderately unstable conditions contribute to this high variation in the flux.

There is negligible difference in the daytime heat flux for most of the cases for flow in the turbine wake or between two turbines (Fig. 5b). The daytime reference flux at NLAE 1 is between 50 and 125 W m$^{-2}$ for most clear-sky conditions. For the southwesterly wind between the B1 and B2 turbine wakes at a distance of about 3.3$D$ the flux difference indicates a small (5–10 W m$^{-2}$) but statistically significant counter gradient downward heat transport when the turbines are in operation. However, when the station is in the wake of turbine B1 there is a similar magnitude but positive upward transport of heat. We believe this result points to the 3-D asymmetry of the turbine wake swirl generated behind the blades: the momentum and heat fluxes also respond to this rotational vortex above the surface. The daytime mean differences in the sensible heat are highly variable among all periods with the turbines OFF and we attribute this behavior in the heat flux to boundary layer-scale mixing (scales of a few hundred to a few thousand meters) as the primary forcing instead of the smaller turbine-scale turbulence.

At night, however, the turbine-scale turbulence (scales on the order of the rotor disk, approximately 80 meters) dominates the ambient boundary layer turbulence having scales of only a few meters. Therefore at night, the turbine influence is distinct, promoting larger downward transport of heat at NLAE 2 (reference flux of −40 W m$^{-2}$). We note weaker downward heat transport (5–10 W m$^{-2}$) within the center of the wakes from turbines B1 and B2 for SSW or the WSW flow condition. Rather, turbine turbulence enhances mixing of heat (by 15–20 W m$^{-2}$) at the edges of the two wakes for the SW direction. All other ON/OFF comparisons outside of this SW window depict flux differences near zero.

#### 4.1.3. Latent heat flux

In contrast to sensible heat flux and momentum flux, the downwind-upwind differences for latent heat flux are ambiguous (Fig. 5a). At night for both the turbines ON and OFF condition, we observe negligible mean change in the transpiration or condensation between NLAE 1 and NLAE 2. However, there is slightly higher variability when the turbines are operational. In the daytime periods, transpiration increases regardless of turbine status. However, like the sensible heat flux, we expect the larger scales of boundary layer mixing to dilute or mask the turbine influence of the fluxes for the bulk of the afternoon hours plotted.

In our refined wake window direction analysis, (Fig. 5b) we clearly see that latent heat flux increases at NLAE 2 by as much as 60 W m$^{-2}$ when it is influenced by the B1 turbine during the DAY condition. We believe that at this distance of 5.5$D$ downstream of

the B1 turbine, the wake is interacting with the surface to increase the canopy flux by about 10–15% or up to 1.0–2.0 mm day$^{-1}$ over the reference flux (350 W m$^{-2}$). A similar examination of the surface mean wind speed difference between the downwind and upwind station reveals over a 0.5 m s$^{-1}$ speed enhancement when the B1 and B2 turbine wakes are influencing the downwind station (figure not shown). We also indicate at NLAE 2 a 5–10% increase in flux in between the B1 and B2 turbine wakes at a distance of about 3.3*D* for the daytime condition. Latent heat differences are highly variable in the daytime OFF cases and we relate our lack of observations to form a statistical interpretation of the data for these large perturbations. For flow between the B2 and B3 turbines however, there is a peculiar result. We detect <10 W m$^{-2}$ reduction of flux in the both the ON and OFF conditions and unfortunately we are unable to link this pattern to any individual factor. We believe there is a combination of three primary atmospheric factors (thermal stability, hub height wind speed, and wind direction) leading to a 0.4 m s$^{-1}$ speed decrease and (6%) reduction in atmospheric conductance at the downwind station. We offer an explanation for one factor in decreasing the latent heat flux, however there may be other physiological factors within the canopy and the soil, which have unknown effects until additional measurements are made within the crop.

At night, there is not a consistent directional factor on the latent heat flux difference. Mean differences are near zero for flow between the B2 and B3 turbine and for the B1 turbine wake in west-south-westerly wind. We are less confident in the southwesterly flow comparisons for the B2 wake and between the B1 and B2 turbines when the turbines are online. However, the sign difference in the flux (12 to −12 W m$^{-2}$) across the B2 wake may indicate flux perturbation by the rotating wake vortex. The OFF condition is near zero for most of the wake sectors except for the B12G case and we refer to our low number of data points as the cause of the high variability. Westerly winds generate larger flux differences than for other directions that indicate the influence of a turbine. Therefore, we suspect that the turbine perturbation of latent heat during the nighttime is secondary to other physiological factors, which were not measured. These physiological factors likely dominate the transpiration or condensation conditions above the crop.

#### 4.1.4. Carbon dioxide flux

We indicated negligible latent heat flux differences between the downwind and upwind station in the previous section and similarly we cannot clearly define CO2 flux differences over the diurnal cycle (Fig. 6a). The $CO_2$ flux differences are less than 0.3 mg m$^{-2}$ s$^{-1}$ (positive at night, negative in the day) both in the ON and OFF conditions. However, there is less variation in the differences particularly for several hours during the nighttime before local midnight and again in the mid morning to early afternoon. The highest variation in the fluxes occurs at the transition stages of the boundary layer a few hours before sunrise and again in the mid afternoon with the maximum wind speed above the boundary layer moving to the surface. Mixing is most vigorous at these times and leads to higher variation than in other day or night periods.

In the daytime and nighttime composites, turbines increase nighttime $CO_2$ respiration by 0.40–0.60 mg m$^{-2}$ s$^{-1}$ at the NLAE 2 station for the south-southwesterly and southwesterly wind direction (Fig. 7b). This category corresponds to a closer downwind distance of turbine B2 (2.8*D* downwind) and for the flow in between the B1 and B2 turbines at 3.3*D* downwind of the turbine line. $CO_2$ flux differences in the OFF cases are near zero except for wind directions between the B1 and B2 turbines, which can be attributed to fewer data points in this directional and turbine status category.

In the day time the edges of the B1 and B2 turbine wakes promote higher $CO_2$ canopy assimilation (0.3–0.4 mg m$^{-2}$ s$^{-1}$) and we

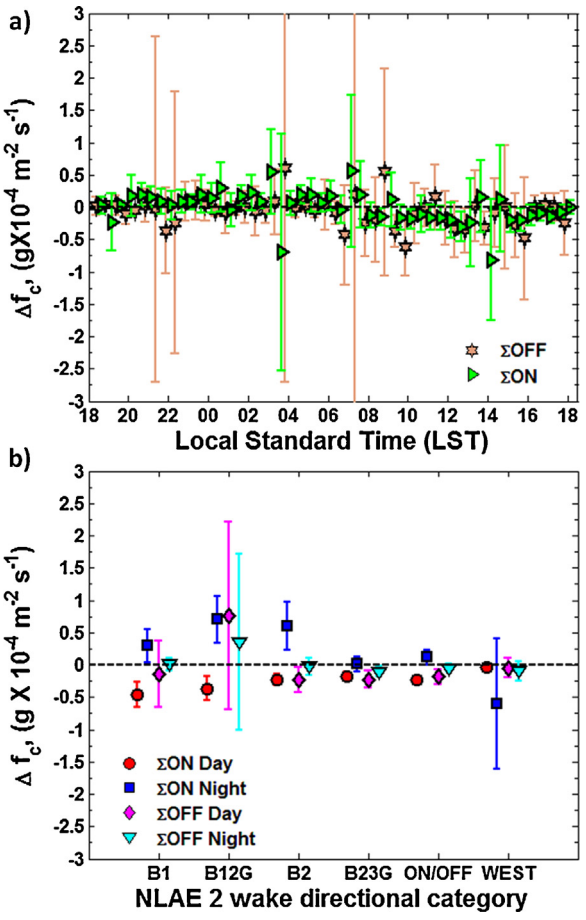


**Fig. 6.** As in Fig. 3 but for $CO_2$ flux ($f_c$).

indicate a slightly larger canopy drawdown (0.5 mg m$^{-2}$ s$^{-1}$) when the B1 turbine wake is over NLAE 2. We believe there is consistent daytime coupling of turbine-enhanced downward turbulent flux of $CO_2$ and upward flux of $H_2O$ for this range of wind directions at approximately 3.0 to 5.5*D* downstream of the turbines. It is important to note that our turbine cases of wake influence demonstrate 50% or greater downward flux than for the southerly flow case between the B2 and B3 turbines and for westerly, non-wake flow. The daytime $CO_2$ fluxes in the ON and OFF states are similar for wind directions between southerly and south-south westerly winds and this may indicate that our flux differences are caused by pressure flow perturbations around the turbine line rather than from the turbine-generated turbulence. Further investigation will help isolate the mechanisms responsible for the flux modification. We recognize that $CO_2$ respiration is both a thermodynamic and dynamic process and so both canopy temperature and soil respiration are important in describing the turbine impact on the $CO_2$ flux. Unfortunately, we did not measure either of these variables and therefore, this partition of the respiration is omitted from the analyses.

### 4.2. Turbulence transfer efficiency difference composites

#### 4.2.1. Friction velocity

We present the turbulence transfer efficiency difference at NLAE 2 according to the same directional sorting metrics for the flux differences as in Figs. 3b, 4b, 5b, and 6b. Only a small range of wind directions indicates that there is a 5–10% increase in turbulence transfer at the downwind tower for the nighttime stable period

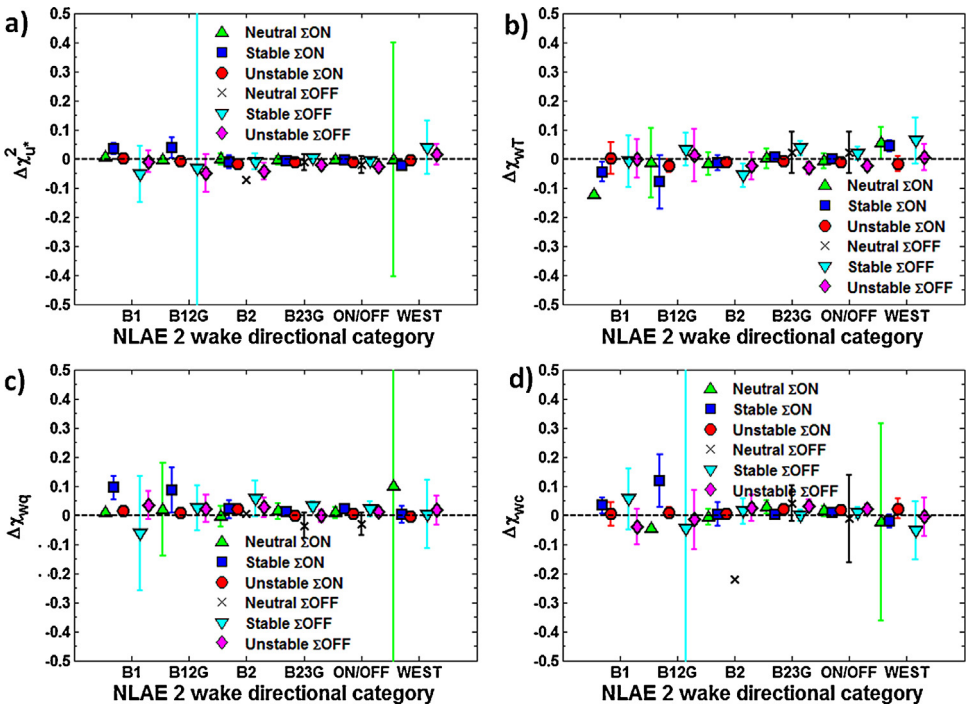


**Fig. 7.** Downwind–upwind mean difference and 95% confidence intervals in turbulence transfer efficiency according to classification by stability categories, turbines ON/OFF, and the turbine wake categories for (a) momentum flux $[u_*^2]$, (b) heat flux $[\overline{w'T'}]$, (c) moisture flux $[\overline{w'q'}]$, and (d) $CO_2$ flux $[\overline{w'c'}]$.

(Fig. 7a). Otherwise, the transfer efficiency is identical upwind and downwind of the tower when the turbines are operational. The highest variability occurs when the turbines are offline and we note a 10% decrease in the turbulence efficiency at NLAE 2 when winds are out of the southwest. This result is surprising but it may indicate that there is a deceleration of the flow from the pressure field perturbation downstream from the turbine. The turbine blades create an obstacle to the flow even when the rotor is not turning. Additional analysis is needed to confirm this conceptual idea.

#### 4.2.2. Sensible heat flux

The turbulence transfer efficiency of heat in Fig. 7b demonstrates alternating increases or decreases at the NLAE 2 station especially in the OFF turbine condition. The only meaningful difference of the flux efficiency in the ON condition is seen in STABLE conditions for southwesterly wind direction indicating a 10–15% increase in turbulence on the edges of the B1 and B2 turbine wakes. Heat is most easily transported in the wake for this condition whereas for southerly to south-south-easterly flow between the B2 and B3 turbine wakes and for wake transport from the B1 turbine, there is little efficiency difference between the two flux stations. As we expect, heat transfer efficiency differences are low in the daytime condition as the scales of turbulence (several hundred meters to a few kilometers) are dominated by buoyant eddies. The turbine scale of mixing is therefore unable to perturb ambient heat flux in this strongly mixed condition.

#### 4.2.3. Latent heat flux

Turbulence transfer efficiencies of moisture are similar at the upwind and downwind station for most directional and stability categories with the turbines ON and OFF. We observe a 10–20% increase in the transfer at NLAE 2 for southwesterly wind for nighttime stable conditions and this is the location on the turbine wake edges from the B1 and B2 turbines (Fig. 7c). A 10% increase in the transfer efficiency is also indicated when the B1 turbine wake influences the downwind station at a distance of 5.5*D*. This pattern is contradictory to the latent heat flux difference as the mean difference is maybe <10 W m$^{-2}$. Through our determination of the turbulence transfer efficiency, we posit that the turbine has the ability to modify nighttime transport of vapor. However, the flux of latent heat is dependent on other factors besides the vertical moisture gradient between the canopy and the atmosphere. Therefore, other studies are warranted to determine the other physiological processes in the crop that are influencing the differences in the latent heat flux.

#### 4.2.4. $CO_2$ flux

In the transfer efficiency of $CO_2$ our results indicate that the turbine-turbulence is only responsible for the perturbation during the nighttime stable conditions and for the southwesterly wind direction (Fig. 7d). We again interpret this difference as the edges of the B1 and B2 turbine wakes facilitate this mixing of carbon dioxide. Similarly as for the transfer of momentum and heat, we relate the blade-sized scales of the turbine-turbulence to be more efficient in modifying the near surface exchanges of $CO_2$ when the ambient turbulence scales are a few to tens of meters.

### 4.3. Spectral analysis of turbine impact on fluxes

#### 4.3.1. Comparison of power spectra

The nighttime spectral analysis of momentum components and vertical heat transport provide clear evidence of the turbine influence at the downwind station. In the power spectra of $v$ ($fS_v/u_*^{-2}$) (Fig. 8a and b) a 50% increase in the peak intensity at the downwind station occurs when the turbines are in operation. The frequency of peak intensity also shifts to smaller-sized eddies at the downwind station, from 0.025 fz/u to near 0.05 fz/u. Similar features occur in the power spectra of $u$ (figure not shown). The spectral differences are negligible when the turbines were off (Fig. 8c and d), although at that time, two hours later, the influence of a nighttime

low-level jet has increased surface wind speed and therefore the velocity variance. While the turbines are OFF, differences between the peak intensity are within 10% and no discernable shifts in the length scale for this peak spectral band emerge.

Our measurements indicate up to an 80% increase in the w-power spectra ($fS_w/u_*^{-2}$) when the turbines are ON. However, there is no clear shift in the turbulent scale of the peak energy portion of the spectrum (figure not shown). For the offline case we observe a negligible station difference in the peak spectral intensity (<10%) and a very small change in the frequency band pertaining to the peak at NLAE 2. The combination of turbine influences in both the horizontal and vertical scales of the energy spectra suggests an influence on the co-spectra of momentum and heat.

#### 4.3.2. Comparison of co-spectra

The vw-co-spectra in Fig. 9a and b also depict higher spectral intensity (by as much as 80%) at the downwind station when the turbines are operational than for when the wind farm is offline (Fig. 9c and d). Enhanced intensity and shifting of the peak energy band to smaller scales from 0.06 fz/u to 0.09 fz/u at the downwind station agree with the higher fluxes reported in Fig. 3 and Fig. 8. In the OFF condition the peak intensity at NLAE 2 is within 5% of NLAE 1, but there may also be a weak shift to larger scales of motion.

The turbine effect is also evident in the turbulent heat flux (Fig. 10a and b). The downwind station has 25% higher spectral peak intensity than the reference station and the energy scale of this peak is also shifted considerably to the right of the ambient station position. However, when the turbines are offline the peak spectral difference between the two stations is within 5% and there is no shift in the energy scale for this band.

## 5. Discussion

Canopy fluxes of momentum, heat, moisture, and carbon dioxide can be modified directly by the enhanced turbulence in the wake, by the reduction of vertical mixing underneath the turbine wake, or by influences of the static pressure field between each line of turbines. Previous analyses (Zhou et al., 2012a and 2012b; Baidya Roy et al., 2004; Baidya Roy, 2011; Baidya Roy and Traiteur, 2010) suggest that wind farm impacts on surface temperatures are most discernible at night. Our results show some evidence in the daytime that a turbine wake can perturb $H_2O$ and $CO_2$ fluxes at a distance of 5.5$D$ downstream. This 5.5$D$ location indicates some expansion of the wake, although it is unlikely that the wake has reached the canopy surface. We report about an 8–12% increase in daytime $CO_2$ penetration from the influence of the B1 or B2 turbines, but this is smaller than the difference of $CO_2$ flux (12–20%) between two corn fields, one irrigated and one dry-land farmed each with a different corn hybrid as reported in Suyker et al. (2004). However, individual events occur when flux perturbations attributed to turbines may match or exceed those related to other field-scale heterogeneities.

Among the $CO_2$ flux differences in the ON and OFF cases, we notice similar magnitudes of the flux difference. One possible explanation of the conflicting results is the flow perturbations around obstacles (e.g. Wang et al., 2001). That is, even motionless turbines in a relatively homogeneous boundary layer likely have some influence on all the energy and $CO_2$ surface fluxes. Our results demonstrate that this perturbation is strongest behind an individual turbine and not across the whole line of turbines. This may indicate that the static pressure field behind each turbine measurably perturbs the flow, regardless of whether the turbines are operational or offline (Rajewski et al., 2013; Smith et al., 2009). Turbine tower shadow effects of over-speeding flow below and between turbine rotors have been previously reported among smaller-scale turbines (e.g. Ainslie, 1988; Whale et al., 1996) and detected recently in Hirth and Schoeder Ka-band radar imagery (2013).

At night, $CO_2$ respiration and sensible heating are enhanced by the turbines when the wake is both directly overhead the flux station at a distance of 5.5$D$ downstream from the turbine or when the outside edge of the wake is above the station at a distance of 2.8–3.3$D$ downstream from the turbine. Our estimates of the nighttime turbine-perturbed heat flux are in reasonable agreement with numerical studies that parameterize the momentum sink and turbulence sources of the turbines (Baidya Roy et al., 2004; Baidya Roy, 2011; Fitch et al., 2012; Fitch et al., 2013a). The representation of the flux differences also is comparable to the scaled wind tunnel experimental results (Chamorro and Porté-Agel, 2010; Zhang et al., 2012, 2013). We observe an increased (more negative) heat flux at NLAE 2 unlike the decreased (less negative) flux demonstrated in the nocturnal LES simulation of Lu and Porté-Agel (2011), noting that the simulation used an infinite turbine array for deep wind farm impacts while we studied the effect of the first row of turbines. It is plausible that for the more oblique wind directions from the southeast or east-southeast our measurements would be responding to a reduction in the scalar flux from the influence of multiple lines of turbines southeast and east-southeast of the CWEX study area.

The spectral analyses substantiate our nighttime flux difference composites presented in the previous two sections. This case study provides a sample of power spectra and co-spectral differences between the upwind and downwind towers whereas other aspects of this data are reserved for future reports. These spectra are difficult to compare with wind tunnel or simulation-generated spectra because those results are focused on the rotor depth above the surface. An increase in the power spectra by up to 6× the ambient are possible within 5.0–10.0$D$ downstream of a turbine (Chamorro and Porté-Agel, 2009; Markfort et al., 2012; Zhang et al., 2012). Conversely, our surface measurements taken at NLAE 2 are only about 2.8$D$ downstream from the B3 turbine and show similarities to the 2–5× increase of the ambient spectra at hub height within a distance of 1$D$ downstream (Crespo and Hernández, 1996). Further spectral analyses (multiple cases for several wind directions and or speeds of the turbine) are needed to better understand the three dimensional asymmetries of the interaction of the turbine-generated turbulence and ambient scales of turbulence.

We find agreement in our results and in our conceptual model of turbine-turbulence more efficiently perturbing the nighttime scales of above-canopy mixing. We provide some insights from previously reported work on the connection to $u_*$ and scalar flux. The wind tunnel studies of Zhang et al. (2012, 2013) report how the aligned turbine arrays give alternating patches of higher (lower) scalar flux on the left (right) cross-wind side of the turbine wakes for daytime boundary layer situations. This may correspond to the downward sweep induced by the blades on the left side of a turbine rotating clockwise and a corresponding upward sweep on the right side of the rotor (e.g. Yang et al., 2012). These upward and downward sweeps would mark the edge of the blade-tip vortices, which undergo expansion and a helical rotation around the downwind side of the turbines to create the turbulence in the wake (Connell and George, 1982). The vortex rotation is opposite of the rotation of the turbine blades to conserve angular momentum. Field detection of these wake vortices from operational turbines is very limited, so our understanding of the structure and evolution of the wake is developed from wind tunnel or numerical simulations.

Zhang et al. (2012) reported that for neutral or convective boundary layer conditions, the tip vortices are present at a distance

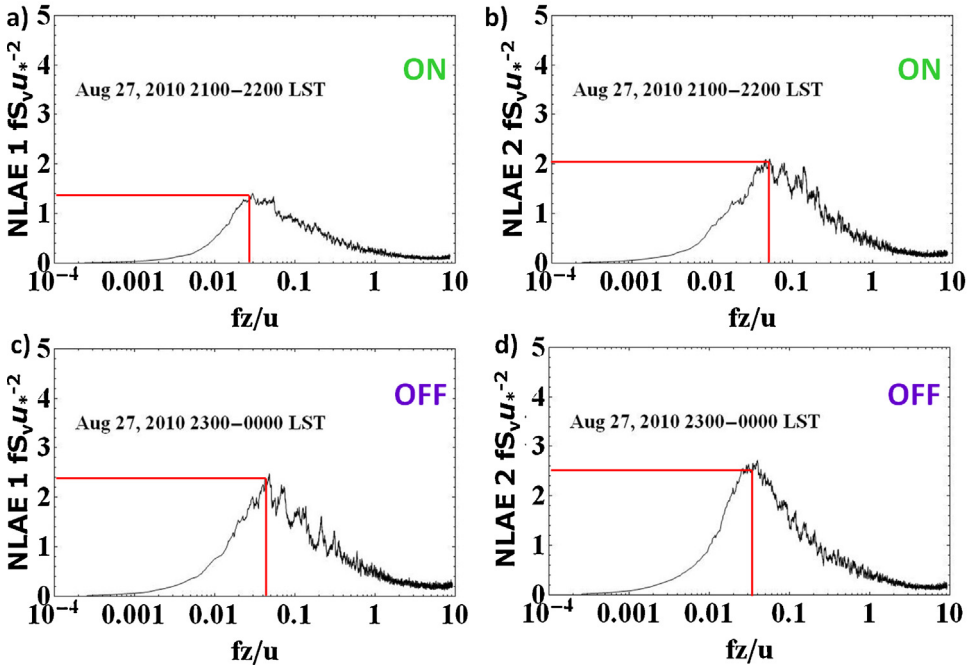


**Fig. 8.** Upwind vs. downwind flux station v-power spectra of momentum for turbines ON period of 21:00–22:00 LST Aug 27, 2010 at (a) NLAE 1 and (b) NLAE 2 and for turbines OFF period of 23:00–00:00 LST August 27–28, 2010 at (c) NLAE 1 and (d) NLAE 2.

of 3*D* downwind of the turbine, whereas by 5*D* there is complete dissipation of these motions. Our field measurements demonstrated some agreement to those daytime findings, yet we believe that some coherent structure of the wake influences the surface fluxes at a distance of greater than 5*D* downwind, at least at night. Under a south-westerly wind direction, NLAE 2 may be influenced by the left side of the B2 turbine wake, and therefore, the sign in the flux difference is not consistent with what we expect inside the wake. Calaf et al., (2011) in their numerical simulations commented on two opposing forces on the sensible heat flux perturbation. In a fully developed turbine-wake boundary layer, the turbine wakes increase $u_*$ beyond the top of the blades ($u_{*\mathrm{hi}}$) whereas below the turbines, the speed reduction in the wake leads to a decrease in the friction velocity ($u_{*\mathrm{low}}$). This ratio of $u_{*\mathrm{hi}}/u_{*\mathrm{low}}$ will control how the scalar flux will change near the surface. We did not observe this effect in our data as we only compared effects on the upwind and downwind side of one line of turbines.

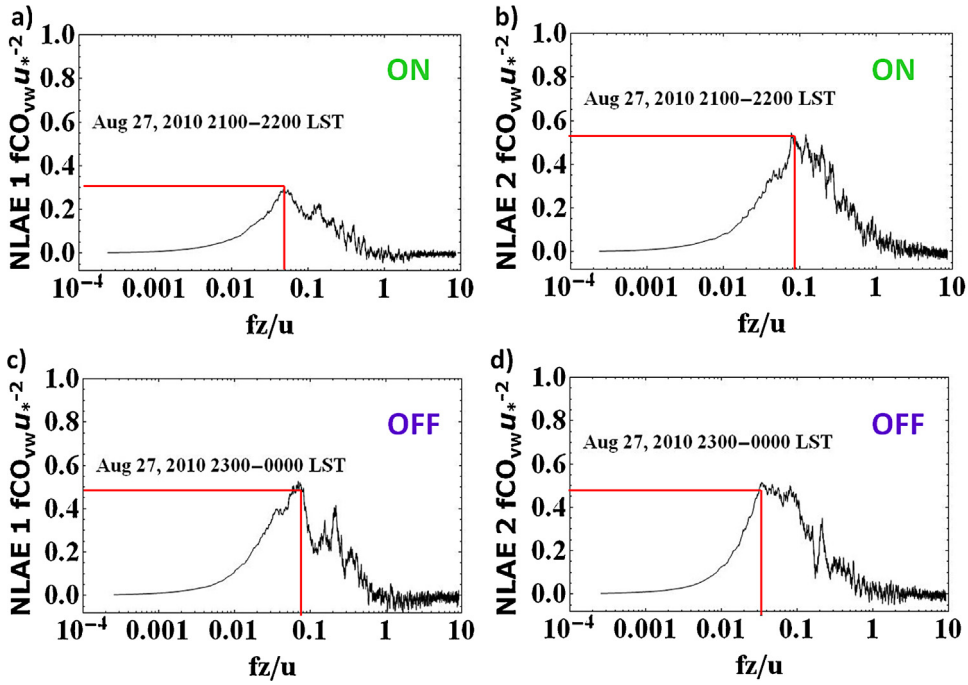


**Fig. 9.** Upwind vs. downwind flux station vw-co-spectra of momentum for turbines ON period of 21:00–22:00 LST August 27, 2010 at (a) NLAE 1 and (b) NLAE 2 and for turbines OFF period of 23:00–00:00 LST August 27–28, 2010 at (c) NLAE 1 and (d) NLAE 2.

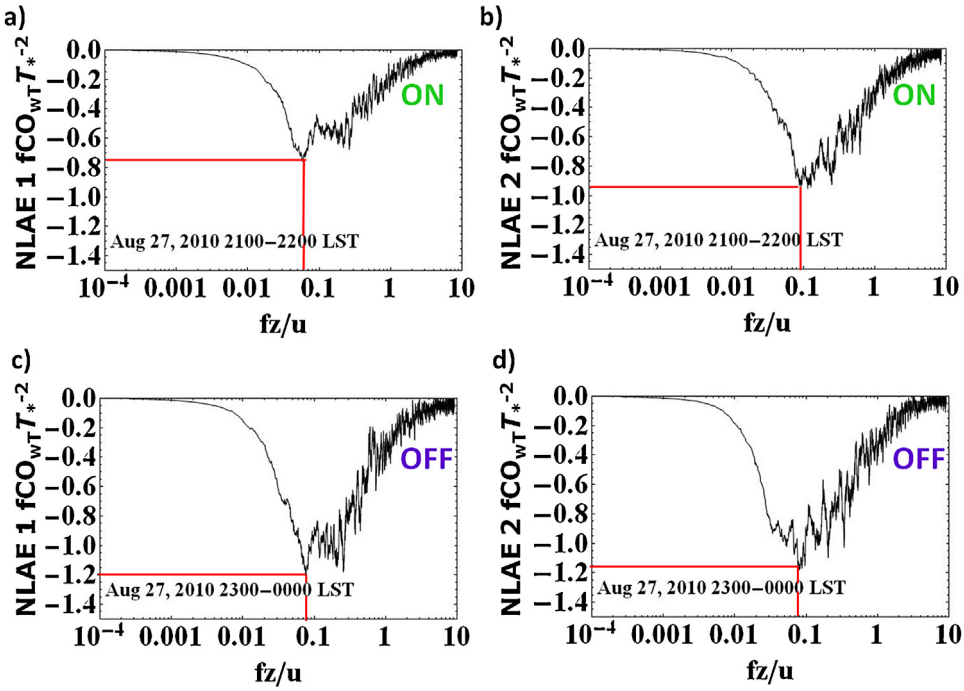


**Fig. 10.** Upwind vs. downwind flux station wT-co-spectra of heat for turbines ON period of 21:00–22:00 LST August 27, 2010 at (a) NLAE 1 and (b) NLAE 2 and for turbines OFF period of 23:00–00:00 LST August 27–28, 2010 at (c) NLAE 1 and (d) NLAE 2.

## 6. Conclusion

Surface fluxes measured upwind and downwind of a line of turbines give evidence of conditional crop microclimate modification by individual wind turbines. Our results show that the turbines did not contribute to sensible heat flux during the day at levels measurably above ambient. Concurrent differences in daytime latent fluxes are significant at a distance of 3–5*D* downstream of a turbine and we have evidence that transpiration may be enhanced at most around 1 mm day$^{-1}$. Daytime $CO_2$ fluxes exhibit a small but not statistically significant enhancement with turbine activity when the turbines are ON as compared to when the turbines are OFF. However, our flux difference comparisons of the ON cases to westerly winds indicate a potentially five-fold increase in $CO_2$ flux at a distance of 5.5*D* downstream of the turbine. Conversely, at night the ambient turbulence is enhanced by the mixing generated from the turbines. Both sensible heat flux and $CO_2$ respiration are increased 1.5–2 times the reference magnitude. We could not discern any major differences in the latent heat flux at night.

Although we observe changes in the $CO_2$ and $H_2O$ fluxes above the canopy, we did not measure biophysical changes within the crop. Therefore we could not determine the overall impact of wind turbines and wind farms on yield. There is weak evidence that the daytime $CO_2$ uptake can be increased for fields that are within a location of 5.5*D* from a turbine, but we have higher confidence that nighttime respiration is enhanced in the lee of the turbine line. Respiration may also be increased by turbines causing a larger pressure pumping of the soil surface and release of $CO_2$ out of the crop canopy (e.g. Takle et al., 2004).

Extrapolating these flux differences after one row of turbines to a large wind farm of several rows is difficult. We expect changes in the turbine mixing as the wind moves through additional turbines within the wind farm. The nonlinear turbulence interactions between multiple wakes could either enhance the effects described here, or the multiple-wake interactions could saturate the effects on fluxes. Future studies would require several measurement systems within and above the crop canopy at multiple locations upwind and downwind of multiple turbine lines to ascertain what physiological and yield impacts are possible from large wind farms. The data presented here suggest two competing effects: an enhanced downward flux of $CO_2$ into the canopy during the daytime and a comparable or higher nocturnal venting of $CO_2$ (via increased mixing and a warmer nighttime temperature) oppose each other and limit the aggregate benefit to corn yield. Although we investigated the grain yield both north and south of the turbine line, the spatial field-scale variability was within ±5 bushels/acre. Quantifying the perceived impact of wind farms on crop yield remains a topic for future field experimentation.

## Acknowledgments

This work was supported in part by the National Renewable Energy Laboratory under Professor Lundquist's Joint Appointment. NREL is a national laboratory of the U.S. Department of Energy, Office of Energy Efficiency and Renewable Energy, operated by the Alliance for Sustainable Energy, LLC. Partial funding for CWEX-10 was provided by the Ames Laboratory (DOE) and the Center for Global and Regional Environmental Research at the University of Iowa. Surface flux stations for CWEX-11 were provided by NCAR Earth Observing Laboratory under an instrumentation deployment, and undergraduate student participation was supplemented by funding from an NSF Research Experience for Undergraduates program under grant 1063048. We recognize Tom Horst, Steve Oncley, and Gordon MacLean from NCAR EOL for their assistance in data-post processing and analysis techniques. The authors also recognize assistance in interpretation of the results from James Brache, Thomas Sauer, Fernando Miguez, and Sotirios Archontoulis. We also recognize Michael Rhodes from CU for editing contributions of the manuscript. Data analysis was supported in part by the National Science Foundation under the State of Iowa EPSCoR Grant 1101284. The authors also acknowledge the wind farm manager and land owners/operators cooperation in conducting CWEX.

We give recognition to one farm manager who shared their yield monitor information for the 2010 growing season. The SCADA data provided by the owner of the meteorological observations within the wind farm was also a beneficial component in conducting this analysis.

## References


Adams, M., Keith, D., 2007. A wind farm parameterization for WRF. Preprints. 8th WRF Users Workshop, Boulder, CO, June 2007 (Available online http://www.mmm.ucar.edu/wrf/users/workshops/WS2007/abstracts/5-5_Adams.pdf. Accessed 22 September 2008).

Ainslie, J.F., 1988. Calculating the flowfield in the wake of wind turbines. J. Wind Eng. Ind. Aerodyn. 27, 213–224.

Aitken, M.L., Rhodes, M.E., Lundquist, J.K., 2012. Performance of a wind-profiling lidar in the region of wind turbine rotor disks. J. Atmos. Oceanic Technol. 29, 347–355, http://dx.doi.org/10.1175/JTECH-D-11-00033.1.

American Wind Energy Association, 2013. U.S. wind industry year-end 2012 market report. (Available online http://www.awea.org/suite/upload/AWEA_USWindInddustryAnnualMarketReport2012_ExecutiveSummary.pdf. Accessed 17 May 2013).

Armstrong, A., Waldron, S., Whitaker, J., Ostle, N.J., 2014, Wind farm and solar park effects on plant–soil carbon cycling: uncertain impacts of changes in ground-level microclimate. Global Change Biol., http://dx.doi.org/10.1111/gcb.12437

Baidya Roy, S., 2011. Simulating impacts of wind farms on local hydrometeorology. J. Wind Eng. Ind. Aerodyn. 99, 491–498, http://dx.doi.org/10.1016/j.jweia.2010.12.013.

Baidya Roy, S., Traiteur, J.J., 2010. Impacts of wind farms on surface air temperatures. Proc. Natl. Acad. Sci. 107, 17899–17904, http://dx.doi.org/10.1073/pnas.1000493107.

Baidya Roy, S., Pacala, S.W., Walko, R.L., 2004. Can large wind farms affect local meteorology? J. Geophys. Res. 109 (D19), 101, http://dx.doi.org/10.1029/2004JD004763.

Barthelmie, R.J., 1999. The effects of atmospheric stability on coastal wind climates. Meteor. Appl. 6, 39–47.

Barthelmie, R.J., Crippa, P., Wang, H., Smith, C.M., Krishnamurthy, R., Choukulkar, A., Calhoun, R.,Valyou, D., Marzocca, P., Matthiesen, D., Brown, G. and Pryor, S.C., 2013. 3D wind and turbulence characteristics of the atmospheric boundary-layer. Bull. Amer. Meteor. Soc., e-view, 130909112657004. http://dx.doi.org/10.1175/BAMS-D-12-00111.1

Barthelmie, R.J., Pryor, S.C., Frandsen, S.T., Hansen, K.S., Schepers, J.G., Rados, K., Schlez, W., Neubert, A., Jensen, L.E., Neckelmann, S., 2010. Quantifying the impact of wind turbine wakes on power output at offshore wind farms. J. Atmos. Oceanic Technol. 27, 1302–1317, http://dx.doi.org/10.1175/2010JTECHA1398.1.

Blanken, P.D., Black, T.A., Yang, P.C., Neumann, H.H., Nesic, Z., Staebler, R., den Hartog, G., Novak, M.D., Lee, X., 1997. Energy balance and canopy conductance of a boreal aspen forest: Partitioning overstory and understory components. J. Geophys. Res. 102 (D24), 28915–28927, http://dx.doi.org/10.1029/97JD00193.

Calaf, M., Parlange, M.B., Meneveau, C., 2011. Large eddy simulation study of scalar transport in fully developed wind-turbine array boundary layers. Phys. Fluids 23, 126603, http://dx.doi.org/10.1063/1.3663376.

Campbell, G.S., Norman, J.M., 1998. An Introduction to Environmental Biophysics, 2nd ed. Springer –Verlag, New York.

Campbell Scientific, Inc., 2014. CSAT3 Three dimensional sonic anemometer instruction manual. 72 pp.(Available online: http://s.campbellsci.com/documents/us/manuals/csat3.pdf. Accessed 11 March 2014).

Cevarich, M., Baidya Roy, S., 2013. Impact of wind farms on surface and air temperatures. Preprints. Fourth Conference on Weather Climate and the New Energy Economy, Austin, TX, January 2013.

Chamorro, L.P., Porté-Agel, F., 2009. A wind-tunnel investigation of wind-turbine wakes: boundary-layer turbulence effects. Bound. Layer Meteorol 132, 129–149, http://dx.doi.org/10.1007/s10546-009-9380-8.

Chamorro, L.P., Porté-Agel, F., 2010. Effects of thermal stability and incoming boundary-layer flow characteristics on wind-turbine wakes: A wind-tunnel study. Bound. Layer Meteorol. 136, 515–533, http://dx.doi.org/10.1007/s10546-010-9512-1.

Connell, J.R., George, R.L., 1982. The wake of the MOD-OA wind turbine two rotor diameters downwind on 3rd December 1981. Report no. PNL-4210, Pacific Northwest Laboratory, Battelle.

Crespo, A., Hernández, J., 1996. Turbulence characteristics in wind-turbine wakes. J. Wind Eng. Indust. Aerodyn. 61, 71–85.

Emeis, S., 2010. A simple analytical wind park model considering atmospheric stability. Wind Energy 13, 459–469, http://dx.doi.org/10.1002/we.367.

Fitch, A.C., Olson, J.B., Lundquist, J.K., Dudhia, J., Gupta, A.K., Michalakes, J., Barstad, I., 2012. Local and mesoscale impacts of wind farms as parameterized in a mesoscale NWP model. Month. Weath. Rev. 140, 3017–3038, http://dx.doi.org/10.1175/MWR-D-11-00352.1.

Fitch, A.C., Olson, J.B., Lundquist, J.K., Olson, J.B., 2013a. Mesoscale influences of wind farms throughout a diurnal cycle. Month. Weath. Rev. 141, 2173–2198 http://dx.doi.org/10.1175/MWR-D-12-00185.1

Fitch, A.C., Olson, J.B., Lundquist, J.K., 2013b. Representation of wind farms in climate models. J. Climate 26, 6439–6458 (accepted for publication) http://dx.doi.org/10.1175/JCLI-D-12-00376.1

Henschen, M., Demchak, K., Herrholtz, B., Rudkin, M., Rhudy, L., Larson, E., Doogs, B., Holland, J., Martin, J., 2011. Do wind turbines affect weather conditions? A case study in Indiana. J. Purdue Undergrad. Res. 1, 22–29, http://dx.doi.org/10.5703/jpur.01.1.4.

Hirth, B.D., Schroeder, J.L., 2013. Documenting wind speed and power deficits behind a utility-scale wind turbine. J. Appl. Meteorol. Climatol. 52, 39–46, http://dx.doi.org/10.1175/JAMC-D-12-0145.1.

Leuning, R., van Gorsel, E., Massman, W., Isaac, P.R., 2012. Reflections on the surface energy imbalance problem. Agric. For. Meteorol. 156, 65–74, http://dx.doi.org/10.1016/j.agrformet.2011.12.002.

Lu, H., Porté-Agel, F., 2011. Large-eddy simulation of a very large wind farm in a stable atmospheric boundary layer. Phys. Fluids 23, 065101, http://dx.doi.org/10.1063/1.3589857.

Markfort, C.D., Zhang, W., Porté-Agel, F., 2012. Turbulent flow and scalar transport through and over aligned and staggered wind farms. J. Turb. 13, N33, http://dx.doi.org/10.1080/14685248.2012.709635.

Meyers, T.P., Hollinger, S.E., 2004. An assessment of storage terms in the surface energy balance of maize and soybean. Agric. For. Meteorol. 125, 105–116.

Moriwaki, R., Kanda, M., Watanabe, T., Turbulent transfer efficiency of momentum, heat, vapor, and $CO_2$ measured in the urban surface layer over a densely built up canopy. Preprints. In 15th Symposium on Boundary Layers and Turbulence, American Meteorological Society, Wageningen, The Netherlands, July 2002.

Pichugina, Y.L., Banta, R.M., Kelley, N.D., 2005. Application of high resolution doppler lidar data for wind energy assessment. Preprints. 2nd symposium of Lidar Atmospheric Applications, San Diego, CA., January 2005.(Available online http://ams.confex.com/ams/pdfpapers/86691.pdf; Accessed 17 March 2010).

Rajewski, D.A., Takle, E.S., Lundquist, J.K., Oncley, S.P., Prueger, J.H., Horst, T.W., Rhodes, M.E., Pfeiffer, R., Hatfield, J.L., Spoth, K.K., Doorenbos, R.K., 2013. CWEX: Crop/Wind Energy Experiment: observations of surface-layer, boundary-layer and mesoscale interactions with a wind farm. Bull. Amer. Meteorol. Soc. 94, 655–672, http://dx.doi.org/10.1175/BAMS-D-11-00240.

Rhodes, M.E., Lundquist, J.K., 2013. The effect of wind turbine wakes on summertime Midwest atmospheric wind profiles. Boundary-Layer Meteorol. 149, 85–103, http://dx.doi.org/10.1007/s10546-013-9834-x.

Roth, M., Oke, T.R., 1995. Relative efficiencies of turbulent transfer of heat, mass, and momentum over a patchy urban surface. J. Atmos. Sci. 52, 1863–1874, http://dx.doi.org/10.1175/1520-0469.

Schotanus, P., Nieuwstadt, F.T.M., DeBruin, H.A.R., 1983. Temperature measurement with a sonic anemometer and its application to heat and moisture fluctuations. Boundary-Layer Meteorol. 26, 81–93.

Smith, C.M., Barthelmie, R.J., Pryor, S.C., 2013. *In situ* observations of the influence of a large onshore wind farm on near-surface temperature, turbulence intensity and wind speed profiles. Environ. Res. Lett. 8, 034006, http://dx.doi.org/10.1088/1748-9326/8/3/034006.

Smith, R.B., 2009. Gravity wave effects on wind farm efficiency. Wind Energy 13, 449–458, http://dx.doi.org/10.1002/we.366.

Storm, B., Basu, S., 2010. The WRF model forecast-derived low-level wind shear climatology over the United States Great Plains. Energies 3, 258–276, http://dx.doi.org/10.3390/en3020258.

Stull, R., 1988. An Introduction to Boundary Layer Meteorology. Kluwer Academic Publishers, Dordecht.

Suyker, A.E., Verma, S.B., Burba, G.G., Arkebauer, T.J., Walters, D.T., Hubbard, K.G., 2004. Growing season carbon dioxide exchange in irrigated and rain fed maize. Agric. For. Meteorol. 124, 1–13, http://dx.doi.org/10.1016/j.agrformet.2004.01.011.

Takle, E.S., Massman, W.J., Brandle, J.R., Schmidt, R.A., Zhou, X., Litvina, I.V., Garcia, R., Doyle, G., Rice, C.W., 2004. Influence of high-frequency ambient pressure pumping on carbon dioxide efflux from soil. Agric. For. Meteorol. 124, 193–206, http://dx.doi.org/10.1016/j.agformet.2004.01.014.

U.S. DOE Office of Energy Efficiency and Renewable Energy, 2008. 20% Wind Energy by 2030: Increasing Wind Energy's Contribution to U.S. Electricity Supply. NREL Report No. TP-500-41869; DOE/GO-102008-2567. 248 pp. (Available online http://www.nrel.gov/docs/fy08osti/41869.pdf. Accessed 27 January 2009).

Vermeer, L.J., Sørensen, J.N., Crespo, A., 2003. Wind turbine wake aerodynamics. Prog. Aero. Scien. 39, 467–510, http://dx.doi.org/10.1016/S0376-0421(03)00078-2.

Walsh-Thomas, J.M., Cervone, G., Agouris, P., Manca, G., 2012. Further evidence of impacts of large-scale wind farms on land surface temperature. J. Renew. Sustain. Energy Rev. 16, 6432–6437, http://dx.doi.org/10.1016/j.rser.2012.07.004.

Wang, C., Prinn, R.G., 2010. Potential climatic impacts and reliability of very large-scale wind farms. Atmos. Chem. Phys. 10, 2053–2061, http://dx.doi.org/10.5194/acp-10-2053-2010.

Wang, H., Takle, E.S., 1995. A numerical simulation of boundary-layer flows near shelterbelts. Boundary-Layer Meteorol. 75, 141–173.

Wang, H., Takle, E.S., Shen, J., 2001. Shelterbelts and windbreaks: Mathematical modeling and computer simulation of turbulent flows. Ann. Rev. Fluid Mech. 33, 549–586.

Webb, E.K., Pearman, G.I., Leuning, R., 1980. Correction of flux measurements for density effects due to heat and water vapour transfer. Q. J. Roy. Meteorol. Soc. 106, 85–100.

Whale, J., Papadopoulos, K.H., Anderson, C.G., Helmis, C.G., Skyner, D.J., 1996. A study of the near wake structure of a wind turbine comparing measurements from laboratory and full-scale experiments. Sol. Energy 56, 621–633.

Wilczak, J.M., Oncley, S.P., Stage, S.A., 2001. Sonic anemometer tilt correction algorithms. Boundary-Layer Meteorol. 99, 127–150.
Yang, Z., Sarkar, P., Hu, H., 2012. Visualization of the tip vortices in a wind turbine wake. J. Visualization 15, 39–44, http://dx.doi.org/10.1007/s12650-011-0112-z.
Zhang, W., Markfort, C.D., Porté-Agel, F., 2012. Wind-turbine wakes in a convective boundary layer: A wind-tunnel study. Boundary-Layer Meteorol. 146, 161–179, http://dx.doi.org/10.1007/s10546-012-9751-4.
Zhang, W., Markfort, C.D., Porté-Agel, F., 2012. Near-wake flow structure downwind of a wind turbine in a turbulent boundary layer. Exp. Fluids 52, 1219–1235, http://dx.doi.org/10.1007/s00348-011-1250-8.
Zhang, W., Markfort, C.D., Porté-Agel, F., 2013. Experimental study of the impact of large-scale wind farms on land–atmosphere exchanges. Environ. Res. Lett. 8, 015002, http://dx.doi.org/10.1088/1748-9326/8/1/015002.
Zhou, L., Tian, Y., Baidya Roy, S., Thorncroft, C., Bosart, L.F., Hu, Y., 2012a. Impacts of wind farms on land surface temperature. Nature Clim. Change 2, 539–543, http://dx.doi.org/10.1038/nclimate1505.
Zhou, L.M, Tian, Y.H., Baidya Roy, S., Dai, Y., Chen, H., 2012b. Diurnal and seasonal variations of wind farm impacts on land surface temperature over western Texas. Clim. Dyn., http://dx.doi.org/10.1007/s00382-012-1485-y, Online publication date: 24 August 2012.